RSC Advances

PAPER

View Article Online
View Journal | View Issue

Cite this: *RSC Adv.*, 2025, **15**, 48109

Fifth-order nonlinear optical properties of through space charge transfer pyridinium salt

Arturs Bundulis, *[a] Kaspars Leduskrasts *[b] and Anete Sapne[a]

Received 25th September 2025
Accepted 27th November 2025

DOI: 10.1039/d5ra07294h

rsc.li/rsc-advances

The fifth-order nonlinear optical (NLO) properties of a through space charge transfer (TSCT) pyridinium organic salt were investigated using the Z-scan technique with a femtosecond laser. Unlike previous studies, focusing on through bond charge transfer molecules and their third-order nonlinear effects, this work presents the first evidence that TSCT designed organic molecules show significant fifth-order nonlinear refraction (n_4) with a negligible third-order nonlinear refraction (n_2) component. The TSCT designed molecule demonstrated weak two-photon absorption (2PA) and a strong fifth-order nonlinear refractive index response, with peak values occurring near 700 nm. The spectral dispersion of the n_4 coefficient correlated with the 2PA spectrum, suggesting a linked electronic mechanism. The measured n_4 values are on the order of 10^{-24} to 10^{-25} cm^4 W^{-2}, comparable to those observed in other high-performance organic NLO materials, but with lower nonlinear optical losses. These findings highlight the potential of TSCT molecules for high-intensity, low-loss photonic and optoelectronic applications where higher-order nonlinearity is advantageous.

Introduction

Nonlinear optical (NLO) materials are central to emerging photonic applications, including ultrafast switching, optical limiting, and advanced microscopy.[1] Purely organic NLO systems are particularly attractive due to their large susceptibilities and the ease of structural functionalization.[2] Current molecular design strategies largely rely on through-bond charge transfer (TBCT), achieved by conjugating donor and acceptor units within aromatic scaffolds (Fig. 1A). Pyridinium-based acceptors, in particular, have been widely employed to enhance charge-transfer efficiency, yielding pronounced third-order NLO responses such as two-photon absorption (2PA) and the Kerr effect.

Experimental studies on TBCT pyridinium systems demonstrate significant variability depending on the excitation regime. Using continuous-wave (CW) lasers, Zidan *et al.* investigated TBCT-quinolinium salts and observed reverse saturable absorption (RSA) with a nonlinear absorption coefficient of $\alpha_2 = 2.15 \times 10^{-3}$ cm W^{-1} and a negative nonlinear refractive index of $n_2 = -1.05 \times 10^{-9}$ cm^2 W^{-1} at 635 nm.[3] Jothi *et al.* employed an fs Z-scan at 1064 nm on TBCT-pyridinium crystals, reporting $\alpha_2 = 5.8 \times 10^{-5}$ cm W^{-1} and $n_2 = -4.1 \times 10^{-10}$ cm^2 W^{-1}, with RSA and self-defocusing attributed to excited-state absorption.[4] Similarly, Wu and Tian studied TBCT-pyridinium derivatives under fs pulses, finding third-order susceptibility values up to 1.0×10^{-7} esu and $n_2 \approx 10^{-9}$ cm^2 W^{-1}, highlighting strong polarizability from intramolecular charge transfer.[5] In the 700–850 nm range, most organics generally exhibit 2PA cross-sections of 100–2000 GM,[5–9] with some of the most efficient systems reaching exceptional values. Wu and Tian reported nonlinear absorption spanning 0.064–1.1636 $\times 10^{-9}$ cm W^{-1} and a maximum 2PA cross-section of 73 695 GM for a pyridinium TBCT system,[5] double the highest values observed in other organic classes, such as molecules peaking near 33 000 GM.[10] In general TBCT pyridinium systems have attracted a lot of attention due to their pronounced third-order nonlinear properties with Kerr effect of order 10^{-9}–10^{-10} cm^2 W^{-1} which is 5-orders of magnitude higher when compared to SiN and SiC.[11,12] Studies of materials incorporating the pyridinium moiety, a well-known acceptor for π-conjugated charge-transfer centered organic molecules, have mainly focused on two-photon absorption and Kerr effect, with some reports on three-photon absorption in near infrared region 1000–1500 nm.[8]

Recently there has been first indications of TBCT-design materials exhibiting fifth-order Kerr effects.[13] Materials exhibiting intense fifth-order nonlinear susceptibilities could offer unique opportunities for ultra-fast all-optical modulation[14] and Soliton generation.[15] The current TBCT-design however is not conducive to achieve this goal, as although higher order nonlinear susceptibility is measurable, the measured third order contribution was 14-orders of magnitude higher than the fifth order contribution.[13] To overcome the 10^{14}-fold gap in nonlinear susceptibilities between lower- and higher-order effects requires a fundamental rethinking of organic molecular design to

[a]*Institute of Solid State Physics, University of Latvia, Kengaraga 8, LV-1063, Riga, Latvia. E-mail: arturs.bundulis@cfi.lu.lv*

[b]*Latvian Institute of Organic Synthesis, Aizkraukles 21, LV-1006, Riga, Latvia. E-mail: kledus@osi.lv*

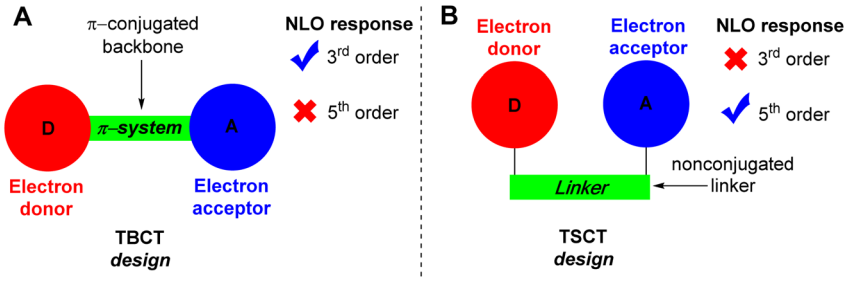

Fig. 1 Schematic TBCT (A) and TSCT (B) designs of organic molecules.

effectively target higher-order nonlinearities. In this work, we depart from the conventional TBCT framework and explore a through-space charge transfer (TSCT) pyridinium system, where the donor and acceptor moieties are located in close spatial proximity (Fig. 1B), with emphasis on its nonlinear optical response, particularly the third- and fifth-order nonlinearities.

Over the past decade, research on fifth-order NLO effects has expanded significantly, with particular emphasis on semiconductors, organic thin films, and conjugated molecular systems.[16–22] Current studies gives highest fifth-order values to inorganic thin films and ferroelectrics with largest reported values reaching up to about 10^{-19}–10^{-24} cm^4 W^{-2} depending on the system with InN $n_4 = 2.1 \times 10^{-19}$ cm^4 W^{-2} reaching the highest value.[17] Organic molecules and complex polymeric structures also demonstrate measurable responses, typically in the range of 10^{-25}–10^{-27} cm^4 W^{-2}.[23] However, most of these materials also exhibit strong third-order response, limiting their applicability for pure fifth-order applications. The small number of materials being studied and lack spectral dispersion of fifth-order effects limits our understanding of fifth-order nonlinear refractive index that needs to be expanded.

Most nonlinear refractive index and absorption coefficient measurements have employed the Z-scan technique.[24] It allows to determine both the magnitude and sign of nonlinearities, and its application to materials exhibiting simultaneous third- and fifth- order processes has been supported by analytical models, such as Gaussian decomposition and generalized propagation equations.[17,18,25–27] These models allow accurate determination of higher-order coefficients when nonlinear refractive index exhibits dependency on laser power or reverses sign at higher intensities.[23,28]

In this work we demonstrate that a TSCT design, where a pyridinium moiety is positioned in spatial proximity to the donor moiety allows to avoid third order nonlinear contribution and directly target the fifth order response (Fig. 1B). The acquired fifth-order nonlinear refractive index spectral dispersion demonstrates that compound **1** could be applicable for photonic applications in first telecommunication window of 800–900 nm.

Experimental section

Materials and sample preparation

The pyridinium perchlorate **1** with a TSCT design was prepared in four steps from 1,8-dibromonaphthalene **2** by sequential Pd-catalyzed Suzuki couplings, *N*-alkylation, and anion exchange. Thus, the dibromide **2** was first coupled with pyridine-4-boronic acid under Pd catalysis to give the corresponding free base, which was protonated with oxalic acid to yield the oxalate salt **3**. A second Suzuki coupling of **3** using 4-phenylboronic acid afforded the free base pyridine **4**, which upon treatment with MeI underwent *N*-alkylation to deliver the pyridinium iodide. Finally, anion metathesis with $AgClO_4$ exchanged iodide for perchlorate, precipitating AgI and affording pure pyridinium perchlorate **1**, after workup. The obtained salt **1** ($M = 395.84$ g mol^{-1}) was a colorless crystalline material, which was characterized by ^{1}H, ^{13}C NMR, IR, HR-MS, EA, and single crystal X-ray diffraction analysis (for details see SI, S3–S5).

The UV-vis absorption of the TSCT pyridinium salt **1** was measured in acetonitrile (MeCN) at *ca.* 10^{-5} M and ambient conditions, using 10 mm light path UV-quartz cuvettes using Edinburgh Instruments FS5 spectrofluorometer. The absorption of **1** was characterized by four distinct absorption bands with maxima at 237, 262, 288 and 355 nm (Fig. 2). The broad absorption band at 355 nm is attributed to the TSCT between the *N*-methylpyridinium and phenyl moieties. The optical band gap of salt **1** was calculated to be 2.98 eV. The constrained geometry of **1** supports an out of plane twist between the naphthalene linker and phenyl/*N*-methylpyridinium moieties in solution, similar to those observed in the X-ray analysis data (Scheme 1). The near-parallel alignment of the phenyl and *N*-methylpyridinium rings, with centroid–centroid separation of 3.57 Å, indicates the presence of a pronounced intramolecular π–π$^+$ interaction (a subset of the wider cation–π interaction class). Notably, such π–π$^+$ interactions are known to promote extremely efficient TSCT between the π-donor and π$^+$-acceptor systems.[29–31]

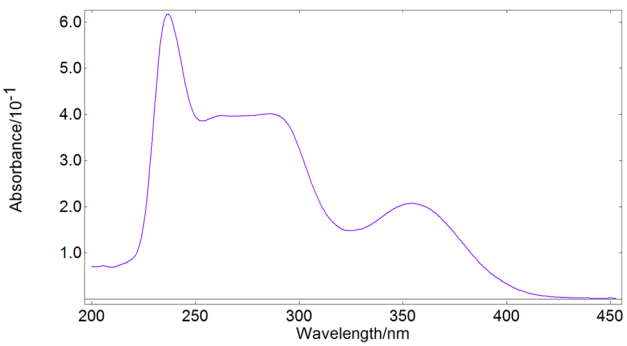

Fig. 2 The linear absorption spectra of **1** in MeCN.

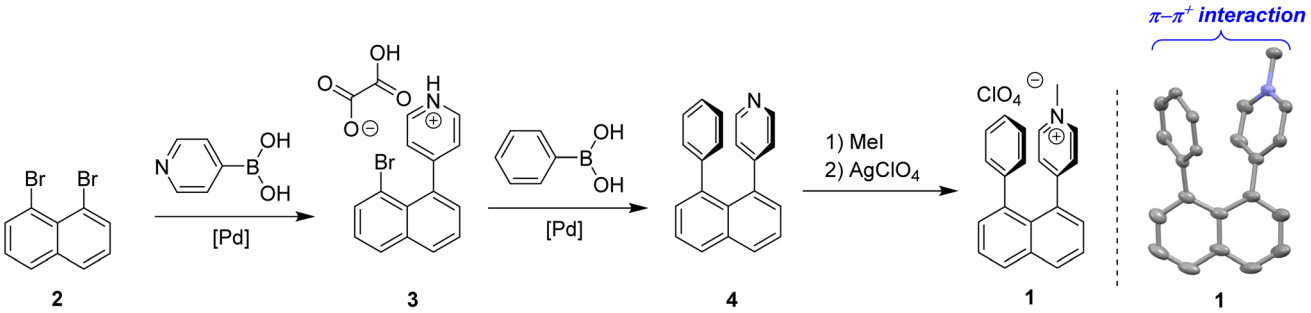

Scheme 1 Synthesis and intramolecular interaction of pyridinium salt **1**.

For NLO measurements synthesized pyridinium salt **1** was dissolved in MeCN with concentration of 0.3 wt%. The solution was contained in a quartz cuvette with a 1 mm light path length.

Z-scan measurement setup

A tunable femtosecond laser system (ORPHEUS-HP pumped by PHAROS PH2) was employed as the excitation source in these studies. The system delivered 150 fs pulses at repetition rates of 500 kHz and, tunable across the 400–1200 nm spectral range. Nonlinear optical properties of the samples were investigated using the standard Z-scan technique. The laser beam was focused using a spherical lens with a 110 mm focal length. The beam waist at focal point varied from 15–20 μm depending on wavelength but ensured thin sample model for 1 mm solutions optical path. The sample was translated along the optical axis through the focal region. Transmitted radiation was recorded using both open-aperture (OA) and closed-aperture (CA) detection schemes to separately characterize nonlinear absorption and nonlinear refraction, respectively. For CA measurements, a 1 mm circular aperture was positioned 200 mm beyond the focal plane, with the CA photodiode detector placed directly behind it. In regions far from the focus, where nonlinear effects are negligible, the normalized transmittance was calibrated to 1. The setup was calibrated using CS_2. Measurements at 800 nm gave $n_2 = (3.50 \pm 0.71) \times 10^{-15}$ cm^2 W^{-1} that fits literature data.[28]

While theoretical models for pure third-order NLO are widely studied, simultaneous third- and fifth- order is less common. In this paper data analysis is based on Bing Gu paper.[32] In case of simultaneous third- and fifth-order NLO effects, refractive index is expressed as:

$$n = n_0 + n_2 \cdot I + n_4 \cdot I^2 \quad (1)$$

where n_0 is linear refractive index of a material, n_2 is third-order nonlinear refractive index, n_4 is fifth-order nonlinear refractive index and I is light intensity. The transmittance function of Z-scan measurements is defined as $T(x, \Phi_{0m})$ that depends on $x = \frac{z}{z_R}$ that is a dimensionless parameter describing sample position normalized to Raileigh length and Φ_{0m} is the phase change of the traveling laser beam induced by the NLO effect $(2m + 1)$th-order expressed as:

$$\Phi_{0m} = k \cdot n_{2m} I^m \cdot L \quad (2)$$

where k is wave number, n_{2m} is NLO refractive index and L is the sample thickness. Third- and fifth- order NLO effect influence on transmittance during Z-scan measurements can be expressed using normalized transmittance $T_1(x, \Phi_{01})$ and normalized transmittance $T_2(x, \Phi_{02})$ respectively:

$$T_1(x, \Phi_{01}) = 1 + \frac{4x\Phi_{01}}{(x^2+1)^2(x^2+9)} + \frac{4(3x^2-5)\Phi_{01}^2}{(x^2+1)^2(x^2+9)(x^2+25)} \quad (3)$$

$$T_2(x, \Phi_{02}) = 1 + \frac{8x\Phi_{02}}{(x^2+1)^2(x^2+25)} + \frac{48(x^2-3)\Phi_{02}^2}{(x^2+1)^4(x^2+25)(x^2+81)} \quad (4)$$

In case of both orders are observed simultaneously an additional mixing parameter needs to be taken into account additional to third- and fifth- order terms from eqn (2) and (3) giving the total transmittance as:

$$T(x, \Phi_{01}, \Phi_{02}) = T_1(x, \Phi_{01}) + T_2(x, \Phi_{02}) + F(x, \Phi_{01}, \Phi_{02}) - 1 \quad (5)$$

where $F(x, \Phi_{01}, \Phi_{02})$ is both order mixing term expressed as:

$$F(x, \Phi_{01}, \Phi_{02}) = \frac{48\Phi_{01}\Phi_{02}(x^4+14x^2-35)}{(x^2+1)^3(x^2+9)(x^2+25)(x^2+49)} \quad (6)$$

In case of two-photon absorption (2PA), material absorption α is expressed as:

$$\alpha = \alpha_0 + \alpha_2 \cdot I \quad (7)$$

where α_0 is linear absorption of a material and $\alpha_2 = \frac{3\pi}{\lambda\varepsilon_0 c n_0^2}\chi_{Im}^{(3)}$ is two-photon absorption.[33] To calculate 2PA coefficient, OA transmission data T is used:

$$T(x) = \sum_{k=0}^{\infty} \frac{(-q)^k}{\frac{1+x^2}{(k+1)^{\frac{3}{2}}}} \quad (8)$$

where parameter q $\alpha_2 \cdot L \cdot I$ includes sample thickness L and laser intensity I_0.

Results and discussion

Open-aperture Z-scan

Pure MeCN samples did not exhibit any observable NLO absorption changes, and all observed OA signal variations were due to the NLO absorption of **1**. The MeCN solution of **1** exhibited weak but measurable 2PA effect. Example of OA measurement at 800 nm is shown in Fig. 3A. Spectral dispersion of 2PA is shown in Fig. 3B.

For better comparison with literature 2PA values were converted to 2PA cross-section values using equation:[34]

$$\sigma_{2PA} = \frac{h\cdot\omega}{N}\cdot\alpha_2 \quad (9)$$

where $h\cdot\omega$ is photon energy and N is molecule concentration per cm^3. Highest value for this compound is 15.9 GM at 800 nm which is low compared to values presented in literature that usually various between 1000–2000 GM with highest values reaching as high as 73 946 GM.[5,6] For practical application this would limit the NLO losses in photonic devices based on this material.

Closed-aperture Z-scan

Pure MeCN measurements were carried out as reference with spectral dispersion of Kerr effect in the 550–950 nm range (Fig. 4). The dispersion follows standard solvent characteristic with slight increase in values at shorter wavelengths.

Closed aperture measurements of **1** displayed unique response that showed a combination of third- and fifth- order effects (see Fig. 5B). The data was fitted with eqn (5) including both third-order and fifth-order contribution. To better understand if pure signal of pyridinium salt **1** exhibits both third- and fifth- order response or only fifth-order pure MeCN signal (see Fig. 5A) was subtracted from solution signal. After this only pure fifth-order effects were observed with no third-order contribution. Resulting signal of pure **1** (see Fig. 5C) was fitted with eqn (5) without the third-order term. This effect had a distinct spectral dispersion. Examples of acquired Φ_{01} for MeCN and

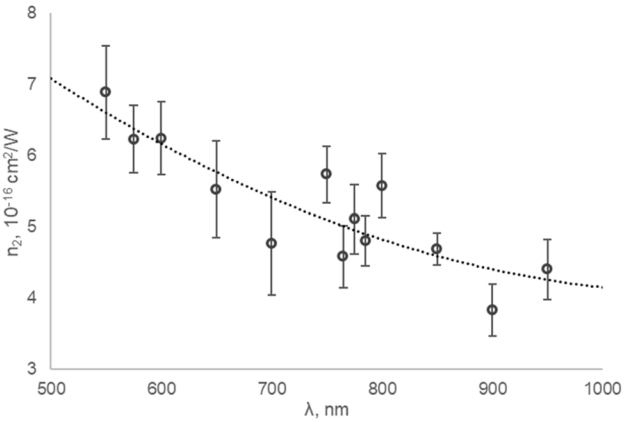

Fig. 4 Spectral dispersion of n_2 values for MeCN.

Φ_{02} of **1** dependence from laser power at 785 nm is shown in Fig. 6.

Fig. 6 indicates that fifth-order strongly dominated the NLO response. Processing data with assumption that both third- and fifth- order effects are present gave $n_2 = 1.03 \times 10^{-14}$ cm^2 W^{-1} at 775 nm which is very low compared to other reports on Kerr effect in pyridinium salts with usual values above $>10^{-10}$ cm^2 W^{-1}.[5] The acquired fifth-order coefficient was calculated to be $n_4 = -1.1 \times 10^{-24}$ cm^4 W^{-1}. The third-order coefficient was calculated through extrapolation of experimental data with no direct experimental observation of third-order response, which is unique in comparison to other studies presenting fifth-order responses. A comparison of various material third- and fifth-order effects is compiled in Table 1. For materials studied around 780–790 nm our studied compound has similar fifth order response to other materials with the difference of an order of magnitude lower third-order response. Compared to other studies where either both third- and fifth- order effects has been observed in single material (similar as in Fig. 5B where we observe third-order contribution from solvent and fifth-order contribution from organic compound)[23] or fifth-order magnitude is calculated through observation of only third-order effect

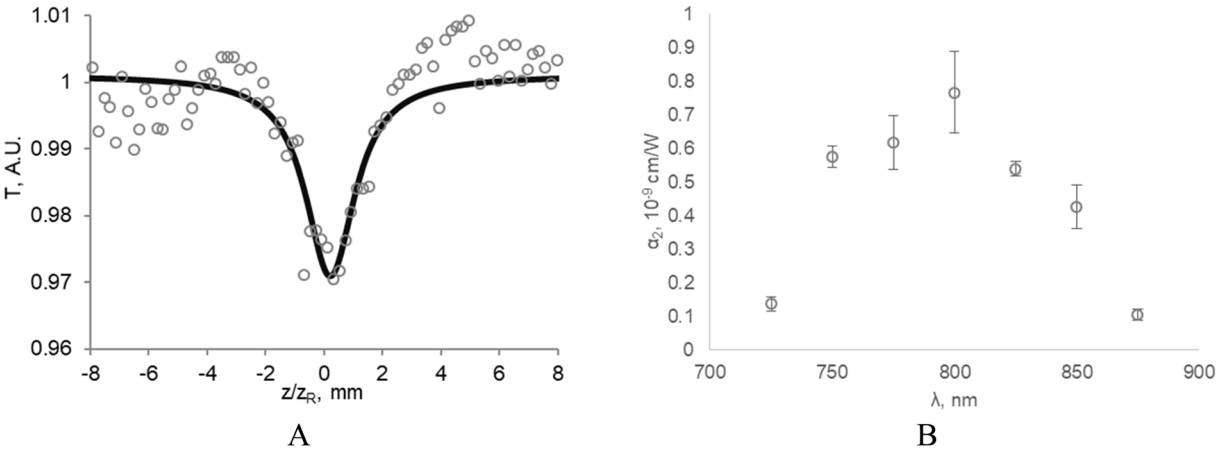

Fig. 3 (A) A standard open-aperture measurement. (B) The 2PA coefficient spectral distribution of **1**.

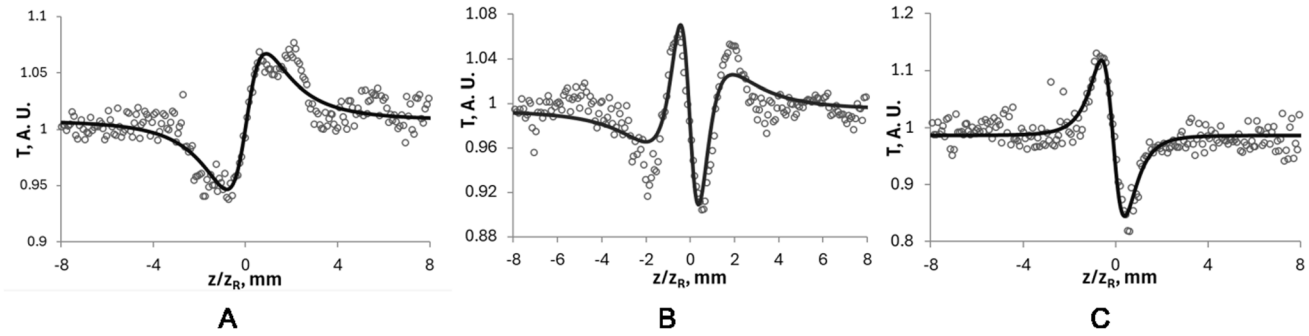

Fig. 5 Closed aperture measurements of MeCN (A) and MeCN+**1** (B). The resulting difference is shown in image (C).

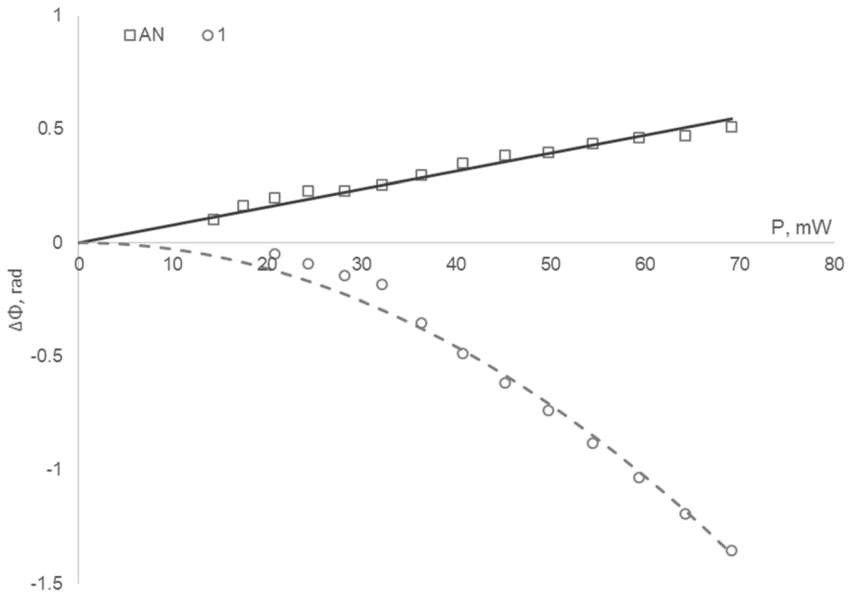

Fig. 6 Induced phase for MeCN (Φ_{01}) and **1** (Φ_{02}).

but with its coefficient dependent on intensity,[22] in this work we observed only fifth-order response and estimation of third-order was based on extrapolation of those data that were close to measurement threshold. As 1% solution was used in experiments the system threshold was 10^{-16} cm^2 W^{-1}. In this comparison we assume that the third-order response of **1** can be estimated to be below the measurement threshold value of $<10^{-14}$ cm^2 W^{-1}, a contribution which is negligible compared to fifth-order response. Amongst other organic material studies C_{60} has reported much higher values but at significantly shorter wavelengths. The increase of fifth-order response at shorter wavelengths has been reported for CS_2.[28]

Table 1 Third- and fifth- order NLO properties of materials

Material	Wavelength, nm	n_2, cm^2 W^{-1}	n_4, cm^4 W^{-2}	References
Salt **1**	785 nm, 150 fs, 500 kHz	$<10^{-14}$	-1.10×10^{-24}	This work
Azobenzene copolymer film	780 nm, 120 fs, 1 kHz	1.54×10^{-13}	-2.06×10^{-24}	22
$Bi_{0.9}La_{0.1}Fe_{0.98}Mg_{0.02}O_3$	780 nm, 350 fs, 1 kHz	2.00×10^{-13}	-2.40×10^{-24}	18
Norbixin	780 nm, 220 fs, 1 kHz	4.43×10^{-16}	-4.65×10^{-27}	23
ZnO	780 nm, 120 fs, 1 kHz	1.00×10^{-13}	-1.40×10^{-26}	21
ZnS	780 nm, 120 fs, 1 kHz	6.90×10^{-14}	3.10×10^{-27}	21
CS_2	1040 nm, 357 fs, 1 kHz	2.10×10^{-15}	-2.00×10^{-27}	28
C_{60}	532 nm, 55 ps, 0.5 Hz	2.1×10^{-10}	1.40×10^{-19}	16
$6PbO–4BaO–20Na_2O–40Nb_2O_5–30SiO_2$	1064 nm, 25 ps, 1 Hz	2.62×10^{-13}	-2.89×10^{-23}	20
InN	800 nm, 100 fs, 82 MHz	-2.50×10^{-11}	2.10×10^{-19}	17

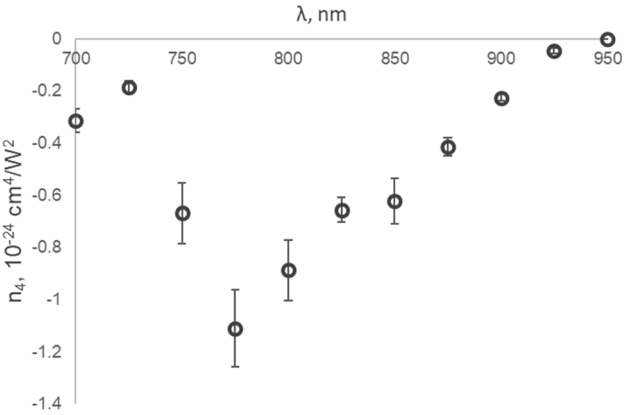

Fig. 7 Spectral dispersion of n_4 values.

Consequently, subsequent calculations were performed under the assumption of a purely fifth-order process. The spectral data reveal a pronounced fifth-order response with a peak near 800 nm (see Fig. 7). The maximum in the n_4 values coincides with the 2PA spectral peak, indicating a clear correlation between the two processes.

This work is the first observation of fifth-order nonlinear refractive effects in pyridinium-based organic salts. As the fifth-order response correlates with 2PA absorption spectrum, its origins could be based on excited state nonlinearities induced by 2PA. Similar observations has been made in case of other organic molecules exhibiting fifth-order effects.[23,35] Acquired values are of similar order of fifth-order NLO effects in other organic compounds in range of 10^{-24}–10^{-25} cm^4 W^{-2}. One of the main differences is very low nonlinear optical losses that are beneficial for various all-optical photonic applications. While there is no widely accepted figures-of-merit (FOM) for fifth-order NLO efficiency we suggest a slightly altered third-order FOM[36] $T = \lambda \cdot \alpha_2/n_2$ of form $T_2 = (\lambda \cdot \alpha_2)^2/n_4$ which is <0.01 over measured spectral range. In the case of third-order material can be applicable for photonic applications if $T < 1$, indicating very good FOM for studied compound. These results demonstrate that the spectral dispersion of n_4 clearly peaks around 800 nm strongly correlating with observed 2PA.

Conclusions

This work presents the first experimental evidence of fifth-order NLO effects in a TSCT-pyridinium organic salt under femtosecond laser excitation. Using Z-scan measurements at wavelengths ranging from 550 to 950 nm, we identified a strong fifth-order nonlinear refractive index (n_4) contribution from the pyridinium salt with negligible third-order contribution. After solvent subtraction, the closed-aperture measurements revealed a peak fifth-order refractive index of $n_4 = -1.1 \times 10^{-24}$ cm^4 W^{-2} near 775 nm, with values remaining above 10^{-25} cm^4 W^{-2} across much of the visible spectrum.

Open-aperture scans indicated weak but measurable two-photon absorption (2PA), with 2PA coefficients α_2 peaking around 7.6×10^{-10} cm W^{-1} near 800 nm with corresponding 2PA cross-section value of 15.9 GM. The spectral overlap of the n_4 and α_2 peaks suggests that excited-state transitions contribute significantly to the fifth-order nonlinearity. To evaluate suitability for photonic devices, we proposed a fifth-order figure-of-merit (FOM) defined as $T_2 = (\lambda \cdot \alpha_2)^2/n_4$. Across the measured spectral range, T_2 values remained below 0.01, significantly lower than the third-order threshold figure-of-merit $T < 1$, indicating excellent performance potential for nonlinear optical systems.

Author contributions

Arturs Bundulis: conceptualization, data curation, formal analysis, investigation, methodology, validation, visualization, writing – original draft, writing – review & editing; Kaspars Leduskrasts: conceptualization, funding acquisition, investigation, methodology, validation, visualization, writing – original draft, writing – review & editing; Anete Sapne: investigation, methodology, validation.

Conflicts of interest

There are no conflicts to declare.

Data availability

The data supporting this article have been included as part of the supplementary information (SI). Supplementary information: compound synthesis, characterization details, and NMR spectra. See DOI: https://doi.org/10.1039/d5ra07294h.

CCDC 2504012 contains the supplementary crystallographic data for this paper.[37]

Acknowledgements

We thank Dr S. Belyakov for X-ray crystallographic analysis. This work was funded by RRF grant No.30/OSI/PG (RRF project No.5.2.1.1.i.0/2/24/I/CFLA/001) and Latvian Quantum Technologies Initiative No. 2.3.1.1.i.0/1/22/I/CFLA/001.

References

1 E. Garmire, *Opt. Express*, 2013, **21**, 30532.
2 D. Dini, M. J. F. Calvete and M. Hanack, *Chem. Rev.*, 2016, **116**, 13043–13233.
3 M. D. Zidan, A. Arfan and A. Allahham, *Opt. Laser Technol.*, 2017, **89**, 137–142.
4 K. Venkatesan, M. Kayalvizhi, L. Jothi and G. Vasuki, *J. Mol. Struct.*, 2022, **1258**, 132687.
5 Y. Tang, H. Liu, H. Zhang, D. Li, J. Su, S. Zhang, H. Zhou, S. Li, J. Wu and Y. Tian, *Spectrochim. Acta, Part A*, 2017, **175**, 92–99.
6 Q.-J. Dong, Z.-B. Cai, L. Ding, P.-H. Luo, Q.-J. He, S.-L. Li, L.-J. Chen, Q. Ye and Y.-P. Tian, *Dyes Pigm.*, 2021, **185**, 108849.
7 D. Shu, D. Wang, M. Li, H. Cai, L. Kong, Y. Tian, X. Gan and H. Zhou, *Dyes Pigm.*, 2021, **194**, 109639.

8 T. He, S. Yao, J. Zhang, Y. Li, X. Li, J. Hu, R. Chen and X. Lin, *Opt. Express*, 2016, **24**, 11091.
9 H. M. Kim and B. R. Cho, *Chem. Rev.*, 2015, **115**, 5014–5055.
10 S.-J. Chung, S. Zheng, T. Odani, L. Beverina, J. Fu, L. A. Padilha, A. Biesso, J. M. Hales, X. Zhan, K. Schmidt, A. Ye, E. Zojer, S. Barlow, D. J. Hagan, E. W. Van Stryland, Y. Yi, Z. Shuai, G. A. Pagani, J.-L. Brédas, J. W. Perry and S. R. Marder, *J. Am. Chem. Soc.*, 2006, **128**, 14444–14445.
11 K. Ikeda, R. E. Saperstein, N. Alic and Y. Fainman, *Opt. Express*, 2008, **16**, 12987.
12 X. Lu, J. Y. Lee, S. Rogers and Q. Lin, *Opt. Express*, 2014, **22**, 30826.
13 C. Wang, C. Fan, C. Yuan, G. Yang, X. Li, C. Ju, Y. Feng and J. Xu, *RSC Adv.*, 2017, **7**, 4825–4829.
14 V. Besse, H. Leblond and G. Boudebs, *Phys. Rev. A*, 2015, **92**, 013818.
15 E. L. Falcão-Filho, C. B. de Araújo, G. Boudebs, H. Leblond and V. Skarka, *Phys. Rev. Lett.*, 2013, **110**, 013901.
16 R. A. Ganeev, M. Baba, M. Morita, A. I. Ryasnyansky, M. Suzuki, M. Turu and H. Kuroda, *J. Opt. A:Pure Appl. Opt.*, 2004, **6**, 282–287.
17 Z. Q. Zhang, W. Q. He, C. M. Gu, W. Z. Shen, H. Ogawa and Q. X. Guo, *Appl. Phys. Lett.*, 2007, **91**, 221902.
18 B. Gu, Y. Wang, W. Ji and J. Wang, *Appl. Phys. Lett.*, 2009, **95**, 041114.
19 A. Saleh, W. Li, H. ALQahtani, M. Neuhaus, A. Alshehri, B. Bergues, M. Alharbi, M. F. Kling, A. M. Azzeer, Z. Wang and A. F. Alharbi, *Results Phys.*, 2022, **37**, 105513.
20 T. Ning, X. Yu, L. Yin and Q. Zhang, *Optik*, 2021, **247**, 167943.
21 J. He, Y. Qu, H. Li, J. Mi and W. Ji, *Opt. Express*, 2005, **13**, 9235.
22 Y. Xue, Y. Wan and B. Gu, *J. Nonlinear Opt. Phys. Mater.*, 2018, **27**, 1850007.
23 N. J. Brito e Silva, F. das Chagas de Melo Brito, T. M. C. M. Baltar, J. L. Magalhães, V. G. F. Viana, F. E. P. Santos and H. A. Garcia, *Results Opt.*, 2022, **6**, 100205.
24 M. Sheik-Bahae, A. A. Said, T.-H. Wei, D. J. Hagan and E. W. Van Stryland, *IEEE J. Quantum Electron.*, 1990, **26**, 760–769.
25 V. Besse, G. Boudebs and H. Leblond, *Appl. Phys. B*, 2014, **116**, 911–917.
26 D. S. Corrêa, L. De Boni, L. Misoguti, I. Cohanoschi, F. E. Hernandez and C. R. Mendonça, *Opt. Commun.*, 2007, **277**, 440–445.
27 G. Tsigaridas, M. Fakis, I. Polyzos, P. Persephonis and V. Giannetas, *J. Phys.:Conf. Ser.*, 2005, **10**, 242–245.
28 V. V. Kim, A. Bundulis, J. Grube and R. A. Ganeev, *Opt. Mater. Express*, 2022, **12**, 2053.
29 K. Leduskrasts, A. Kinens and E. Suna, *Chem. Commun.*, 2023, **59**, 6905.
30 K. Leduskrasts and E. Suna, *ChemistryOpen*, 2021, **10**, 1081.
31 K. Leduskrasts, A. Kinens and E. Suna, *Chem. Commun.*, 2019, **55**, 12663.
32 B. Gu, J. Chen, Y.-X. Fan, J. Ding and H.-T. Wang, *J. Opt. Soc. Am. B*, 2005, **22**, 2651.
33 R. del Coso and J. Solis, *J. Opt. Soc. Am. B*, 2004, **21**, 640.
34 B. Gu, W. Ji, P. S. Patil and S. M. Dharmaprakash, *J. Appl. Phys.*, 2008, **103**, 103511.
35 B. Gu, W. Ji, X.-Q. Huang, P. S. Patil and S. M. Dharmaprakash, *Opt. Express*, 2009, **17**, 1126.
36 E. V. García Ramírez, S. A. Sabinas Hernández, D. Ramírez Martínez, G. Díaz and J. A. Reyes Esqueda, *Opt. Express*, 2017, **25**, 31064.
37 CCDC 2504012: Experimental Crystal Structure Determination, 2025, DOI: 10.5517/ccdc.csd.cc2q1ml0.